Active Wave Computing on Silicon: Chip Experiments

Cs. Rekeczky*, I. Petrás*, I. Szatmári*, and P. Foldesy*

Abstract – **This paper discusses analogic cellular array architectures that can also be used to approximate partial differential equations (PDEs). Cellular arrays are massively parallel computing structures composed of cells placed on a regular grid. These cells interact locally and the array can have both local and global dynamics. The software of this architecture is an analogic algorithm that builds on analog and logical spatio-temporal instructions of the underlying hardware, that is, a locally connected cellular nonlinear network (CNN, [1]-[5]). Within this framework several classes of "wave-type" PDEs could be approximated. Examples will be shown for cellular wave-computing phenomena on existing CNN Universal Machine (CNN-UM, [2]) chips (e.g. [3]-[5]).**

1 INTRODUCTION

It is well known that all PDEs can be approximated to any desired accuracy by introducing finite differences (and possibly discrete variables), i.e. they can always be mapped to a cellular structure. On the other hand, cellular arrays are computationally universal ([9]-[11]) and from an engineering point of view, they can be considered as dedicated architectures for building a universal parallel computer. In a recent summary we have discussed the engineering view that an efficient parallel PDE MACHINE, which can be built, must be a cellular array (see e.g. [3]-[5]). In the sequel we will consider PDE approximations leading to wave-based phenomena on single and multiple-layer cellular array architectures.

2 APPROXIMATING PDES: SINGLE-LAYER WAVE-COMPUTING

Let us consider the following local PDE (a generalized reaction diffusion-type equation class):

$$\frac{\partial \phi(x,y,t)}{\partial t} - div(grad(\phi(x,y,t))) = \Im_1(\phi_0(x,y,t_0)) + \Im_2(\phi(x,y,t)) \quad (1)$$

where ϕ is the image intensity, ϕ_0 represents the initial state and $\Im_1(.)$ and $\Im_2(.)$ are nonlinear functions.

Assuming that the right hand side of (1) is zero we obtain the linear diffusion equation (at steady state the Laplace equation has to be solved). Dropping only the $\Im_2(.)$ term results in a constrained linear diffusion equation ($\Im_1(.)$ calculates a "spatial constrain"). If $\Im_2(.) \approx$ sigm(.) then a trigger-wave (or when $\Im_1(.) \neq 0$ a constrained trigger-wave) equation can be derived.

Using a finite difference approach all these equations naturally map to a cellular structure described by nonlinear ODEs (a CNN architecture). Let us consider an approximation that leads to existing architectures [3]-[5]:

$$\begin{aligned} &\frac{d\phi_{ij}(t)}{dt} = g(\phi_{ij}(t)) - c_1\phi_{ij}(t) \\ &+\frac{c_1}{4}(\phi_{i-1\,j}(t) + \phi_{i+1\,j}(t) + \phi_{ij-1}(t) + \phi_{ij+1}(t)) + z_{ij} \\ &\phi_{ij}(t) = f(x_{ij}(t)) \wedge g(.) = c_0 f(.) \wedge z_{ij} = z_0 + \sum_{kl \in N_1} b_{kl}\phi_{0,kl} \end{aligned} \quad (2)$$

where $\Im_2(.)$ is replaced by $g(.)$, $f(.)$ is a sigmoid-type function and $\Im_1(.)$ is replaced by z_{ij} a linear combination of the input in the nearest neighborhood (plus an offset z_0). By adjusting the parameters c_0, $c_1 \geq 0$ one can obtain different qualitative (e.g. linear diffusion or nonlinear trigger-wave) behaviors [6], [7]. Some experimental results can be found in Fig. 1-2. While diffusion based filters can be primarily used in noise filtering, trigger-waves [7] provide a good approximation to some basic operations of differential morphology [8]. The example in Fig. 2. shows how flat dilation, erosion and reconstruction can be implemented dynamically by these simple nonlinear waves (see also nonlinear wave metrics [6]).

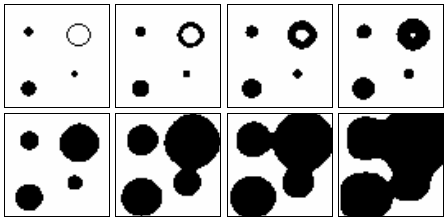

Figure 1: Trigger-wave generation from initial patches: a snapshot of the expanding wave front.

Figure 2 Trigger-waves generate multi-scale flat dilation and erosion operations of differential morphology.

* Analogical and Neural Computing Laboratory, CARI-HAS, Budapest, Hungary
e-mail: rcsaba@sztaki.hu, tel.: +36 1 2796123.

Breaking the "synaptic" positivity, symmetry or isotropy in formulation (1) leads to patterns other than simple binary patches (stripes, checkers, etc.).

3 APPROXIMATING PDES: MULTIPLE-LAYER WAVE COMPUTING

Let us consider the following PDE formulation of a coupled vector valued nonlinear reaction-diffusion system (examples for nonlinear PDEs could be found in [18]):

$$\begin{aligned}
&\frac{d}{dt}\phi_1(\vec{x},t) - div[c_1(\vec{x},t)\ \ grad(\phi_1(\vec{x},t))] = \\
&\qquad \alpha_1(\phi_1(\vec{x},t)) + \beta_1(\phi_1(\vec{x},t_0)) + \gamma_1(\phi_2(\vec{x},t)) \\
&\frac{d}{dt}\phi_2(\vec{x},t) - div[c_2(\vec{x},t)\ \ grad(\phi_2(\vec{x},t))] = \\
&\qquad \alpha_2(\phi_2(\vec{x},t)) + \beta_2(\phi_2(\vec{x},t_0)) + \gamma_2(\phi_1(\vec{x},t)) \\
&\phi_1(\vec{x},t_0) = \phi_{10}(\vec{x}); \qquad c_1(\vec{x},t) = g(\mid grad(\phi_1(\vec{x},t)) \mid) \\
&\phi_2(\vec{y},t_0) = \phi_{20}(\vec{x}); \qquad c_2(\vec{y},t) = g(\mid grad(\phi_2(\vec{x},t)) \mid)
\end{aligned} \tag{3}$$

where $[\phi_1(\vec{x},t)\ \phi_2(\vec{x},t)]$ can be interpreted as the time evolution of a vector valued image intensity ($[\phi_{10}(\vec{x})\ \phi_{20}(\vec{x})]$ is the original image), the vector $\vec{x}$ represents the spatial coordinates, the time variable t can also be interpreted as the scaling parameter and c is the conductance parameter in the diffusion term. The right hand side of the equations consists of three reaction terms: (i) $\alpha(.)$ is the "self-reacting term"; (ii) $\beta(.)$ is a "spatial constraint" (calculated from the initial data); and (iii) $\gamma(.)$ is the "cross-coupling" term. Some proposed functions for $g(.)$ are ([14]):

$$\begin{aligned}
&g_1 = \exp\left(-\mid grad(I(\vec{x},t)) \mid^2 / K^2\right),\ K>0 \\
&g_2 = \left(1+\left(\mid grad(I(\vec{x},t)) \mid / K\right)^{1+\alpha}\right)^{-1},\ \alpha>0, K>0
\end{aligned} \tag{4}$$

Decoupling the two equations ($\gamma_1 = \gamma_2 = 0$) and choosing $\alpha(\xi) = -\xi$ the PDE formulation is given in the form of the so-called "biased" nonlinear anisotropic diffusion equation (Nordström [15]) an extended version of the Perona-Malik formulation [14]. Gerig et. al [16] first proposed the application of coupled nonlinear diffusion systems for vector-valued image processing that has been further studied by many others [18]. For our purposes – motivated by silicon implementation – we focus on a simplified version of (3) fixing the diffusion parameter to a constant value.

In two spatial dimensions and assuming $c = const.$ and (3) reduces to:

$$\begin{aligned}
&\frac{d}{dt}\phi_1(x,y,t) - c_1\, div[grad(\phi_1(x,y,t))] = \\
&\qquad \alpha_1(\phi_1(x,y,t)) + \beta_1(\phi_1(x,y,t_0)) + \gamma_1(\phi_2(x,y,t)) \\
&\frac{d}{dt}\phi_2(x,y,t) - c_2\, div[grad(\phi_2(x,y,t))] = \\
&\qquad \alpha_2(\phi_2(x,y,t)) + \beta_2(\phi_2(x,y,t_0)) + \gamma_2(\phi_1(x,y,t))
\end{aligned} \tag{5}$$

After spatial discretization using the finite difference approach one obtains:

$$\begin{aligned}
&\frac{d\phi_{1,ij}(t)}{dt} = \gamma_1(\phi_{2,ij}(t)) + \alpha_1(\phi_{1,ij}(t)) - c_1\phi_{1,ij}(t) + \\
&\qquad \frac{c_1}{4}(\phi_{1,i-1j}(t) + \phi_{1,i+1j}(t) + \phi_{1,ij-1}(t) + \phi_{1,ij+1}(t)) + \beta_1(\phi_{10,ij}) \\
&\frac{d\phi_{2,ij}(t)}{dt} = \gamma_2(\phi_{1,ij}(t)) + \alpha_2(\phi_{2,ij}(t)) - c_2\phi_{2,ij}(t) + \\
&\qquad \frac{c_2}{4}(\phi_{2,i-1j}(t) + \phi_{2,i+1j}(t) + \phi_{2,ij-1}(t) + \phi_{2,ij+1}(t)) + \beta_2(\phi_{20,ij})
\end{aligned} \tag{6}$$

Finally, with $\alpha(.) = \alpha_0$ and $\beta(.) = \beta_0$ a simplified form (with spatial symmetry and isotropy) of the CNN complex cell equation ([19], [20]) is derived:

$$\begin{aligned}
&\frac{d\phi_{1,ij}(t)}{dt} = \gamma_1\phi_{2,ij}(t) + (\alpha_1 - c_1)\phi_{1,ij}(t) + \\
&\qquad \frac{c_1}{4}(\phi_{1,i-1j}(t) + \phi_{1,i+1j}(t) + \phi_{1,ij-1}(t) + \phi_{1,ij+1}(t)) + z_{1,ij} \\
&\frac{d\phi_{2,ij}(t)}{dt} = \gamma_2\phi_{1,ij}(t) + (\alpha_2 - c_2)\phi_{2,ij}(t) + \\
&\qquad \frac{c_2}{4}(\phi_{2,i-1j}(t) + \phi_{2,i+1j}(t) + \phi_{2,ij-1}(t) + \phi_{2,ij+1}(t)) + z_{2,ij} \\
&z_{1,ij} = \beta_1\phi_{10,ij} + z_1; \qquad z_{2,ij} = \beta_2\phi_{20,ij} + z_2
\end{aligned} \tag{7}$$

Making ϕ_{ij} explicitly depend on a state variable ξ_{ij} such as $\phi_{ij} = f(\xi_{ij}) = sigm(\xi_{ij})$ leads a good approximation to the full-range CNN circuit model ([5], $sigm(.)$ could be a piece-wise linear or monotonic continuous smooth function playing the role of a signal-limiter). The form of the corresponding 2nd order CNN template is as follows:

$$\begin{aligned}
&A_{11} = \begin{bmatrix} 0 & c_1/4 & 0 \\ c_1/4 & \alpha_1 - c_1 & c_1/4 \\ 0 & c_1/4 & 0 \end{bmatrix}; \\
&A_{12} = \gamma_1; B_{11} = \beta_1; \tau_1 = 1; z_1 = 0 \\
&A_{22} = \begin{bmatrix} 0 & c_2/4 & 0 \\ c_2/4 & \alpha_2 - c_2 & c_2/4 \\ 0 & c_2/4 & 0 \end{bmatrix}; \\
&A_{21} = \gamma_2; B_{22} = \beta_2; \tau_2 = 1; z_2 = 0
\end{aligned} \tag{8}$$

Analysis: It should be noted that the diagonal terms could also be added resulting in a much better spatial isotropy during the diffusion process. Symmetry and spatial isotropy of these templates are due to the fact that there are no convection terms ([12]) in the original formulation. With these modifications the sign and magnitude of the template entries in (8) could be changed in any spatial directions. The time constant is also fixed and equal for the two layers. Having two different time variables (say $t'' \neq t'$) in (7) leads to a "double time-scale" descritized system $t''/t' = \tau_2/\tau_1 \neq 1$ that has a practical relevance looking at various second order models.

There is a number of parameter settings of special interest that lead to very different qualitative

behaviors in this symmetric second order system. We have primarily examined and explored the following simple cases ([20], see the appendix for wave-computing examples):

(i) trigger-wave generation (diffusion process in"saturation" at various speeds)

$c1 > 0$; $c2 > 0$; $\alpha1-(c1+1)>0$; $\alpha2-(c2+1)>0$; $\gamma1 = \gamma2 = 0$; $\beta1 = \beta2 = 0$; $\tau2 / \tau1 \neq 1$

(ii) traveling-wave, spiral-wave and auto-wave generation (spatially interacting trigger-waves)

$c1 > 0$; $c2 > 0$; $\alpha1-(c1+1)>0$; $\alpha2-(c2+1)>0$; $\gamma1 \neq 0$; $\gamma2 \neq 0$; $\beta1 \neq 0$; $\beta2 = 0$; $\tau2 / \tau1 \neq 1$

(iii) retina effects (spatially interacting receptive fields)

$\alpha1 \approx c1 >0$; $\alpha2 \approx c2 > 0$; $\gamma1 > 0$; $\gamma2 < 0$; $\beta1 \neq 0$; $\beta2 \neq 0$; $\tau2 / \tau1 \neq 1$

4 CONCLUSIONS

In this paper it has been discussed and illustrated how a reaction-diffusion class of PDEs can be approximated on analogic cellular architecture. The focus has been put on formulations not exceeding the synaptic and algorithmic complexity that can be directly mapped and tested on available CNN-UM chip prototypes (e.g. ACE4K [3], CACE1k [5]). Currently measurement efforts are on-going using the ACE16k [4] CNN-UM chip.

REFERENCES

[1] L. O. Chua and L. Yang, "Cellular Neural Networks: Theory and Applications", *IEEE Trans. on Circ. & Syst.*, Vol. 35, pp. 1257-1290, 1988.

[2] T. Roska and L. O. Chua, "The CNN Universal Machine", *IEEE Trans. on Circ. & Syst.*, Vol. 40, pp. 163-173, 1993.

[3] S. Espejo, R. Domínguez-Castro, G. Liñán, Á. Rodríguez-Vázquez, "A 64×64 CNN Universal Chip with Analog and Digital I/O", *in Proc. ICECS'98*, pp. 203-206, Lisbon 1998.

[4] G. Liñán, R. Domínguez-Castro, S. Espejo, A. Rodríguez-Vázquez, "ACE16k: A Programmable Focal Plane Vision Processor with 128 x 128 Resolution", ECCTD '01, pp.: 345-348, August, Espoo, 2001.

[5] R. Carmona, F. J. Garrido, R. D. Castro, S. Espejo, A. R. Vázquez, Cs. Rekeczky, and T. Roska, "A Bio-inspired 2-layer Mixed-signal Flexible Programmable Chip for Early Vision*", IEEE Transactions on Neural Networks*, to appear.

[6] I. Szatmári, Cs. Rekeczky, T. Roska: "A Nonlinear Wave Metric and its CNN Implementation for Object Classification", *Journal of VLSI Signal Processing*, Vol.23. No.2/3. pp.437-448, Kluwer, 1999.

[7] Cs. Rekeczky and L. O. Chua: "Computing with Front Propagation: Active Contour and Skeleton Models in Continuous-Time CNN", *Journal of VLSI Signal Processing*, Vol.23. No.2/3. pp.373-402, Kluwer, 1999.

[8] P. Maragos, "Differential Morphology and Image Processing", *IEEE Trans. on Image Processing*, Vol. 5, No. 6, 1996.

[9] T. Toffoli, "Computation and Construction Universality of Reversible Cellular Automata", *J. Comput Systems Sci.*, Vol. 15, p. 213, 1977.

[10] L. O. Chua, T. Roska, and P. L. Venetianer, "The CNN is as Universal as the Turing Machine", *IEEE Trans. on Circuits and Systems*, Vol. 40, pp. 289-291, April 1993.

[11] T. Toffoli, "Cellular Automata as an Alternative to (Rather than an Approximation of) Differential Equations in Modeling Physics", *Physica 10D*, pp. 117-127, 1984.

[12] C. Serpico, G. Setti, P. Thiran, and A. Pascarelli, "Local Diffusion, Global Propagation and Propagation Failure in 1-D Cellular Neural Networks", *in Proc. NOLTA'99*, pp. 399-402, Hawaii 1999.

[13] T. Kozek and T. Roska, "A double time-scale CNN for solving 2-D Navier-Stokes equations", *International Journal of Circuit Theory and Applications*, Vol. 24, pp. 49-56, 1996.

[14] P. Perona and J. Malik, "Scale-Space and Edge Detection Using Anisotropic Diffusion", IEEE Trans. on Pattern Analysis and Machine Intelligence, Vol. 12, pp. 629-639, July 1990.

[15] N. Nordström, "Biased Anisotropic Diffusion - A Unified Regularization and Diffusion Approach to Edge Detection", Image Vision Computers, Vol. 8, No 4, pp. 318-327, July 1990.

[16] G. Gerig, O. Kübler, R. Kikinis, and F. A. Jolesz, "Nonlinear Anisotropic Filtering of MRI Data", IEEE Transactions on Medical Imaging, Vol. 11, No. 2, June, 1992.

[17] F. Catté, P. L. Lions, J. M. Morel, and T. Coll, "Image Selective Smoothing and Edge Detection by Nonlinear Diffusion", SIAM Journal on Numerical Analysis, Vol. 29, No. 1, pp. 182-193, 1992.

[18] B. M. H. Romeny (ed.), Geometry-driven Diffusion in Computer Vision, Kluwer Academic Publishers, 1994.

[19] Cs. Rekeczky, T. Serrano-Gatarredona, T. Roska, and A. Rodríguez-Vázquez, "A Stored Program 2nd order/3-layer Complex Cell CNNM-UM", *CNNA 2000*, pp. 213-218, Catania, May 2000.

[20] I. Petrás, Cs. Rekeczky, R. Carmona, T. Roska, and A. R. Vázquez, "Exploration of complex dynamic phenomena in a 32×32-cells stored program 2-layerCNN Universal Machine Chip Prototype with 7-bits Analog Accura", *IEEE Journal on Circuits, Systems and Computers*, to appear.

APPENDIX

Trigger wave generation on the CACE1k chip ([20]):

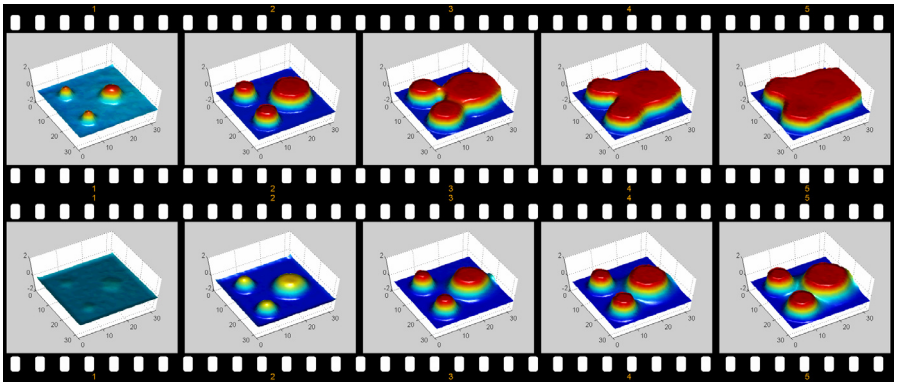

Traveling wave generation on the CACE1k chip ([20]):

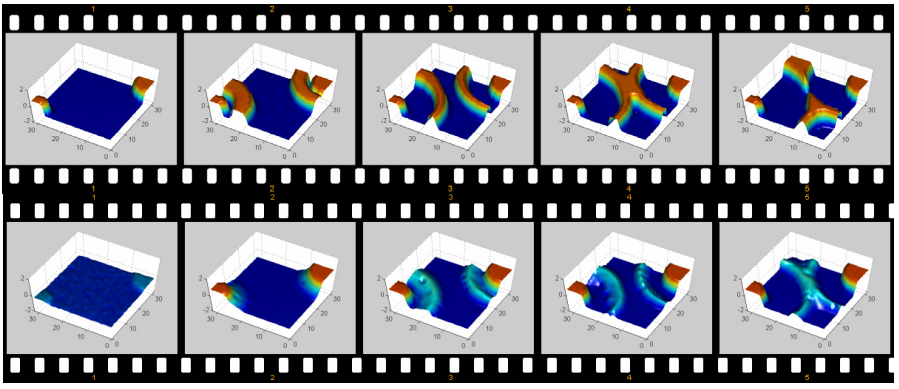

Auto wave generation on the CACE1k chip ([20]):